

Effect of reflow temperature and substrate roughness on wettability, IMC growth and shear strength of SAC387/Cu bonds

Kiran N. Bhat · K. N. Prabhu · Satyanarayan

Received: 23 October 2013 / Accepted: 29 November 2013 / Published online: 6 December 2013
© Springer Science+Business Media New York 2013

Abstract The effect of reflow temperature and substrate surface roughness on wettability, intermetallics and shear strength of Sn–3.8Ag–0.7Cu solder alloy on copper (Cu) substrate was studied. It was found that increase in reflow temperature and substrate surface roughness improved the wettability of solder alloy. The size of needle shaped Cu₆Sn₅ IMCs (intermetallic compounds) increased with increase in temperature. The morphology of IMCs transformed from long to short needles with increase in substrate roughness. Shear strength and shear energy of the solder bond on rough Cu surfaces were found to be higher than that on smooth Cu surfaces. However, the sheared surfaces of the solder bond on rough Cu surface exhibited a transition ridge characterised by sheared IMCs whereas solder bond on smooth Cu surfaces exhibited completely ductile failure. Although, rough surface exhibited higher shear strength and shear energy, smoother surface is preferable due to its predominant bond failure in the solder matrix.

1 Introduction

The harmful effects of toxic Pb on human health and environment have forced the microelectronic industries to stop the usage of Pb in soldering [1]. Among the various lead free solders available, the major lead free solder alloy compositions are eutectic and near eutectic Sn–Ag, Sn–Cu and Sn–Ag–Cu (SAC) systems. In the year 2000, NEMI

(National Electronics Manufacturing Initiative) recommended the replacement of eutectic Sn–Pb by eutectic SAC alloy for reflow soldering [2]. Family of SAC alloys have become most promising lead free solder alloys for modern electronic packaging applications, due to their improved mechanical properties and better solderability as compared to Sn–Pb base solders [3]. Due to the rise in the usage of portable electronic device and products, demand for the device miniaturization, wider application of SMT (Surface Mount Technology) and service environment requirements have given rise for the importance of the solder joint reliability [4]. The solder joints are repeatedly subjected to mechanical loadings during handling, manufacturing, transportation and usage. The mechanical properties of solder joint like shear and fatigue strength, creep resistance are vital issues for solder joint reliability [5].

Sn–3.8Ag–0.7Cu (SAC 387) is one of the eutectic SAC solder alloy widely used in electronic packaging industry. Jiun et al. [6] investigated the mechanical and thermal properties of SAC (SAC 387, SAC 105, SAC 305 and SAC 405) solder alloys and concluded that, SAC 387 is the most favorable solder alloy with highest shear strength, narrow melting point and low surface oxidation. A comparative study of SAC 405 and SAC 387 alloys in terms of alloy properties, solder ball surface morphology, solder ball shear strength, intermetallic compound thickness (IMC) and solderability was carried out and it was concluded that, SAC 387 solder alloy has better solder joint performance [7]. Song et al. [8] assessed the solder joint reliability of SAC 305, SAC 387 and SAC 405 using high-speed ball shear/pull test and board level drop testing. The study revealed that at high speed shear and high pull test, the solder joint produced brittle fracture. Pang et al. [9] investigated the mechanical properties of SAC 387 bulk solder and solder joint (lap joint) at different temperature

K. N. Bhat · K. N. Prabhu (✉) · Satyanarayan
Department of Metallurgical and Materials Engineering,
National Institute of Technology Karnataka, Surathkal,
Mangalore 575 025, India
e-mail: prabhukn_2002@yahoo.co.in

(25, 75 and 125 °C) with different strain rates respectively. The mechanical strength of SAC 387 solder was found to decrease with increase in temperature and increased with increase in the strain rate. Che et al. [10] investigated the IMC growth and morphology of SAC 387 solder alloy under isothermal aging at 125 °C for up to 500 h for plastic ball grid array (PBGA) packages. The morphology of interfacial IMC changed from initial needle-type, transitional scallops + needles and finally to planer type with aging time. The thickness of IMC layer also increased with aging and thermal cycling fatigue life decreased significantly with increase in IMC thickness.

The mechanical properties of solder joints are very sensitive to the wetting of solders and thickness of the IMC layers formed at the interface of the solder joint. However, wettability of solder in soldering process depends on multiple factors such as flux, process temperature, substrate surface roughness and substrate finishing (coating), in addition to intermetallic compounds formation and dissolution [11–15]. Bozack et al. [16] investigated the influence of surface segregation on wetting of SAC series (SAC105, 205, 305, and 405) solder alloys and reported that wetting of solder alloys to board finishes is directly influenced by surface segregation of low-level bulk alloy impurities. The major segregating impurities are C and O at the molten solder alloy surface. The impurities form a high-surface-tension shell around the alloy and inhibit chemical reaction with the substrate, resulting in poor wettability. The interior of poorly wetted droplets of alloy is composed of pure alloy material, which allows for varying amounts of good wetting and spreading depending on the contacting materials [16]. Wetting kinetics of Sn, eutectics of Sn–Ag, Sn–Cu and Pb–Sn was studied by Zhao et al. [17] using a hot-stage microscopy system under a controlled atmosphere. Four-stages of wetting kinetics for eutectic Pb–Sn solder and two stages for lead-free solders on a Cu substrate were identified in their work. Effect of solderability on PCB boards with different surface roughness was studied [18]. It was concluded that horizontally oriented surface roughness reduces wetting force compared to vertically oriented scratches.

In electronic applications the typical bumping targets (substrates) exhibit a range of surface roughness, from $R_a = 0.06 \mu\text{m}$ for Under Bump Metallization (UBMs) on wafers to around $R_a = 0.5 \mu\text{m}$ for the contact pads on Ball Grid Array (BGA) substrates. However, the wetting between depositing solder droplet and substrate (target) surface is a transient phenomenon [19]. Studies on the effect of surface roughness on transient droplet–surface wetting are scant.

A limited research work has been carried out on the effect of surface roughness on wettability of solder alloy [18–22]. It was reported that, higher surface roughness

improves the wettability of the solder alloy [18, 22]. However, a study on the mechanical integrity of solder bond on smooth and rough Cu substrate has not yet been carried out. To assess whether the roughness of bumping targets in the range of 0.06–0.5 μm for UBMs on wafers and contact pads on BGA, is beneficial or not, it is essential to evaluate the mechanical integrity of solder bond on smooth and rough surfaces.

In present study, effect of reflow temperature and substrate surface roughness on wetting characteristics, interfacial intermetallic compounds and shear strength of SAC 387 solder on Cu substrate is investigated.

2 Experimental

The commercial eutectic Sn–3.8Ag–0.7Cu (SAC 387) solder alloy procured from Hybrid Metals, Bangalore was used in the present study. The procured solder rectangular bar of SAC 387 alloy (14 × 19 mm) was drawn into solder wires having a diameter of about 1.4 mm. Solder wires were melted using solder station (KLAPP 920D) and solidified as balls of weight 0.080 gm. Rolled round bar of EC grade copper (99.9 % purity) procured from Hi Tech Sales Corporation, Mangalore was used for making copper substrates ($\varnothing 12.5 \text{ mm} \times 8 \text{ mm}$). The solder balls were then reflowed on Cu substrates having two different surface roughnesses (smooth and rough) at three different temperatures (240, 260 and 280 °C). The substrates were polished using SiC papers of different grit sizes (1/0–4/0 grade), followed by velvet cloth disk polish using diamond-lapping compound to obtain smooth surface finish. Rough surface finish on substrates was achieved using P 120 grade SiC papers. The surface profiles of substrates were assessed using Form Talysurf 50 surface profiler. For smooth Cu surfaces, measured roughness values were found to be in the range of 0.015–0.031 μm and for rough Cu surfaces, the roughness values were in the range of 0.57–0.72 μm . Contact angle measurements were carried out using FTA 200 dynamic contact angle analyzer. The system can capture both static and dynamic spreading phenomena. Spherical ball of solder alloy was kept on the substrate and the solder/substrate system was kept inside the soldering environmental chamber after coating the substrate surface with flux (Inorganic acid, Alfa Aesar, USA). The initial heating rate obtained with the chamber was about 3–4 °C/min, which eventually reduces as the chamber temperature approaches the set value. The spreading process was recorded for approximately for 40 min. The captured images were analyzed using FTA 32 Video 2.0 software to determine the wetting behavior of solder. The solder drop bonded to the substrate was sectioned along the axis and polished using SiC papers of different grit sizes. The final polishing was carried out on

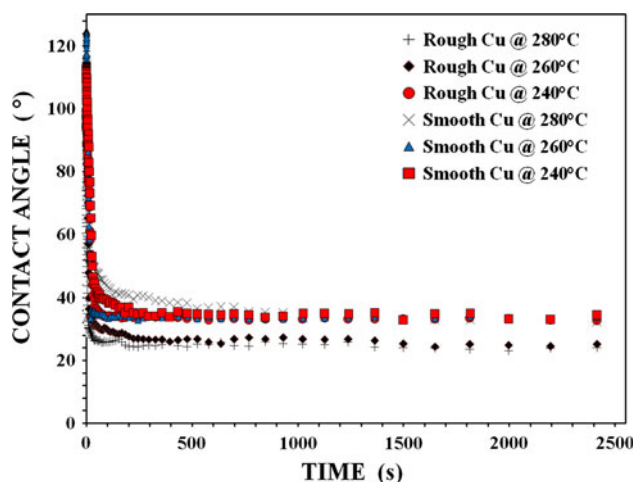


Fig. 1 Spreading behavior of solder alloy on smooth and rough Cu substrate at different reflow temperatures

velvet cloth disc polisher using diamond lapping compound and then etched with 5 % nital (a mixture of C_2H_5OH and conc. HNO_3 in the ratio of 95:5) for about 3–5 s. Zeiss stereomicroscope (Stemi 2000-C) was used for macroscopic view of the sessile drop of solder and Scanning Electron Microscopy (SEM, JEOL JSM 6380LA) was used for microstructural study.

The shear test was performed on solder droplet samples by using the bond tester (Nordson DAGE 4000Plus). As per JESD22-B117A standard, the shear tool stand off should be no greater than 25 % (10 % preferred) of the solder ball height and tool shear speed should be typically in the range of 100–800 μm for low speed shear test. Hence, in the present investigation, the height of shear tool and the shear speed were set at as 3 μm and 200 $\mu m/s$ respectively. The force -displacement curve was recorded during the shear test. Shear test was performed at least two times to find the strength of the solder joint. After the ball shear test, the sheared surfaces were investigated using Zeiss stereomicroscope and scanning electron microscopy (SEM, JEOL JSM 6380LA) with energy disperse spectroscopy (EDS) in Back Scattered Electron mode.

3 Results and discussion

The typical spreading curves of SAC 387 solder on Cu substrates with varying surface roughness and reflow temperatures are presented in Fig. 1. Each experiment was repeated at least two times. During spreading of solder alloy on smooth and rough substrate surfaces at three reflow temperatures, the decrease in contact angle was sharp at the beginning and almost ceased after a period of about 100 s. Equilibrium contact angles obtained on smooth and rough

substrate surfaces at three reflow temperatures are given in Table 1. It was found that increase in surface roughness of Cu surface and increase in reflow temperature enhanced the wettability and spread area of SAC 387 solder alloy. Measured spread areas of the solder alloy after spreading experiment are given in Table 1. The asperities and grooves on rough surface may act as preferable sites for adsorption, reaction, diffusion and nucleation for the solidification of molten solder as the rough surface provides an additional interfacial area for the spreading of liquid solder. This additional surface area provided by the rough surface results in the increase of surface energy due to which wettability of solder alloy improved [23].

It is known that, viscosity and surface tension are dependent on temperature. At higher reflow temperatures, the viscosity and surface tension of solder alloy reduces leading to improvement in the flow characteristics and wettability of the solder. Figures 2 and 3 graphically represent the relationship between the reflow temperature and wettability of the solder alloy.

Interfacial SEM micrographs for the solder alloy solidified on smooth and rough substrate surfaces at three reflow temperatures are shown in Figs. 4 and 5 respectively. Figures show the formation of needle shaped IMCs at the interface of solder/substrate regions. Average length and average thickness of these needles shaped IMCs formed at the solder/substrate interface were measured and reported in Table 2. At higher reflow temperatures, IMCs become longer at the interface of solder/smooth Cu region. The formation of needle shaped IMCs at the interface are dependent on the reflow temperature due to diffusion-controlled process. EDS analysis confirmed that needle shaped IMCs were from the Cu_6Sn_5 phase. Precipitates of needle/plate type Ag_3Sn were also observed in the solder matrix.

At the interface of solder/rough-Cu region, the size of needle shaped Cu_6Sn_5 IMCs also became longer as the reflow temperature is increased. However, these IMCs were shorter than that were observed at the interface of solder/smooth Cu region. Intermetallic compounds that were formed at the interface of solder alloy solidified on rough Cu surface were slightly thicker at higher reflow temperature compared to that observed on smooth Cu surface. At lower reflow temperatures (240 and 260 $^{\circ}C$), the thickness of needle shaped IMCs observed at the interface of solder alloy solidified on smooth and rough Cu surface was found to be nearly similar. Asperities on rough Cu substrate act like capillary tubes. During spreading, the molten solder alloy penetrates into these asperities first and further continues to spread. The penetration of molten solder occurred to a greater degree on the rough surface with asperities completely filled with molten solder. As a result IMCs grew inside asperities also. Hence, the size of the IMCs was shorter and slightly thicker at the solder/

Table 1 Effect of reflow temperature and substrate surface roughness on wettability and shear force of solder alloy on Cu surfaces

Nature of polished Cu surface	Reflow Temp. (°C)	Surface roughness (R _a , μm)	Contact angle (°)	Solder spread area (mm ²)	Shear force (N)	Avg. (N)	Area under curve (J)	Avg. (J)	Shear energy per unit area (J/mm ²)
Mirror	280	0.015	32	25.74	486.56	469	0.715	1.314	0.028
		0.016	31	26.33	451.31		1.914		0.073
	260	0.014	34	23.65	425.14	413	1.434	1.449	0.061
		0.022	30	27.03	401.61		1.465		0.054
	240	0.031	35	24.21	320.31	365	0.992	1.194	0.041
		0.015	34	25.76	410.3		1.397		0.054
Rough	280	0.692	23	25.9	527.03	499	1.396	1.603	0.054
		0.635	24	29.81	470.44		1.811		0.061
	260	0.726	25	24.93	407.31	430	1.174	1.55	0.047
		0.671	25	27.36	454.19		1.927		0.070
	240	0.703	33	23.90	420.6	406	1.728	1.602	0.072
		0.488	30	24.68	392.05		1.476		0.060

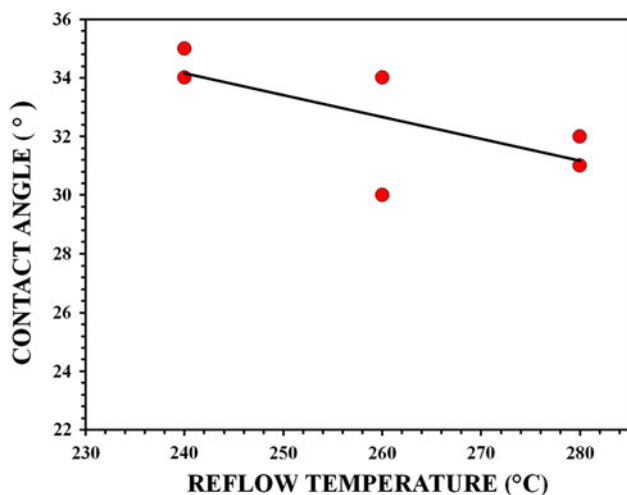


Fig. 2 Contact angle versus reflow temperature for the solder on smooth Cu substrate

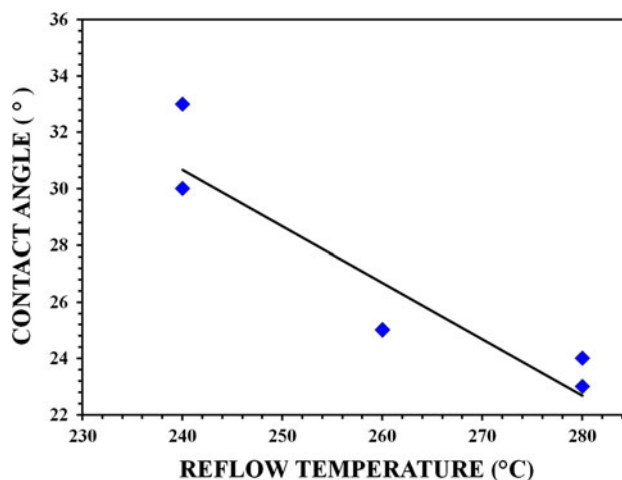


Fig. 3 Contact angle versus reflow temperature for the solder on rough Cu substrate

rough-Cu substrate interface compared to that with solder/smooth Cu interface region. Thick plate like Ag₃Sn precipitates were observed together with Cu₆Sn₅ IMCs at the interface of solder/rough Cu region.

At lower reflow temperatures, there was no sufficient growth of needle shaped IMCs. This is due to the dissolution of smaller amounts of Cu atoms from the substrate into the liquid solder. At higher reflow temperatures, dissolution of Cu atoms from the substrate into the molten solder and vice versa occurred in larger proportion. Hence, IMCs became sufficiently thicker.

The macroscopic images (top view) of the droplets of solder alloy on smooth and rough Cu substrates after the spread and shear test are shown in Figs. 6 and 7 respectively. The solder reflowed on smooth and rough surfaces

at different reflow temperatures were subjected to shear test. The shear force values obtained from the bond tester are presented in Table 1. It was observed that, the maximum shear strength value of solder bond increased with increase in reflow temperature on both smooth and rough Cu substrates. However, average shear force values of solder bond on rough Cu was found to be higher than that on smooth Cu surface. Figures 8 and 9 show the force versus displacement curves corresponding to SAC 387 solder obtained during shear test on smooth and rough Cu substrates reflowed at different temperatures.

Figure 10a, b show the SEM images of fractured surfaces of solder droplet reflowed at 280 °C on smooth and rough substrates. SAC 387 solder solidified on smooth Cu surface exhibited ductile mode of failure with shear marks

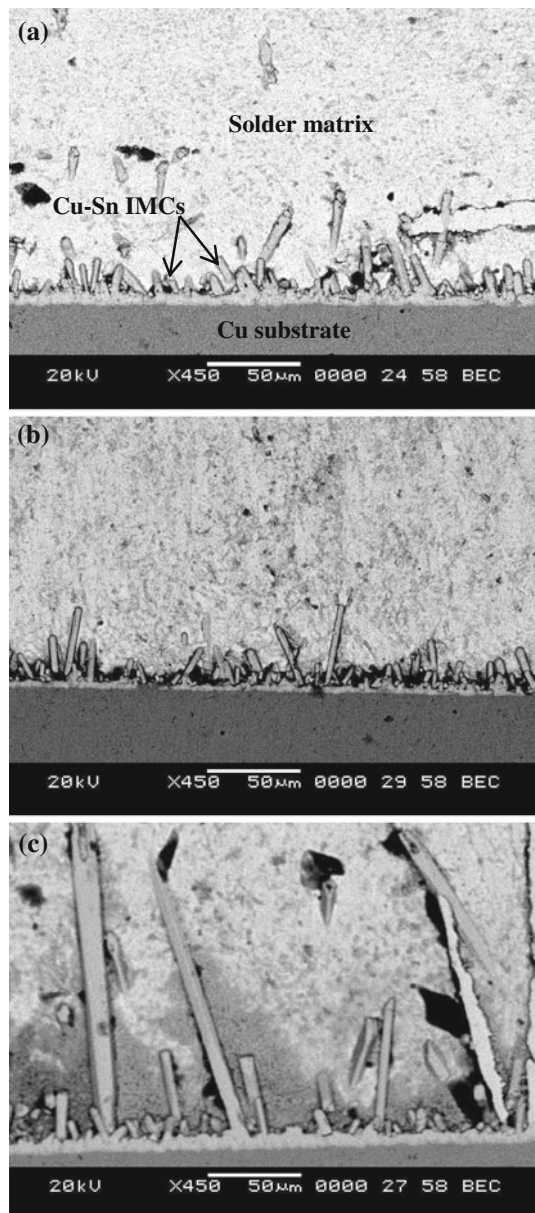


Fig. 4 SEM micrographs of solder solidified on smooth Cu surface at **a** 240 °C, **b** 260 °C and **c** 280 °C reflow temperatures

on the fractured surface (Fig. 10a). However, the fractured surfaces on rough Cu surfaces showed a transition ridge (Fig. 10b) where the shear failure mode shifts from solder to the interface. A similar behavior (ductile failure mode on smooth Cu and ridge on rough surface) was observed for the spreading of solder alloy on Cu surfaces at different reflow temperatures. The shear marks indicated that the fracture occurred predominantly in the bulk of the solder matrix whereas the transition ridge indicates that fracture occurred at the solder/substrate interface.

The ternary eutectic SAC 387 alloy is strengthened by the precipitation of Cu_6Sn_5 and Ag_3Sn IMC particles in the

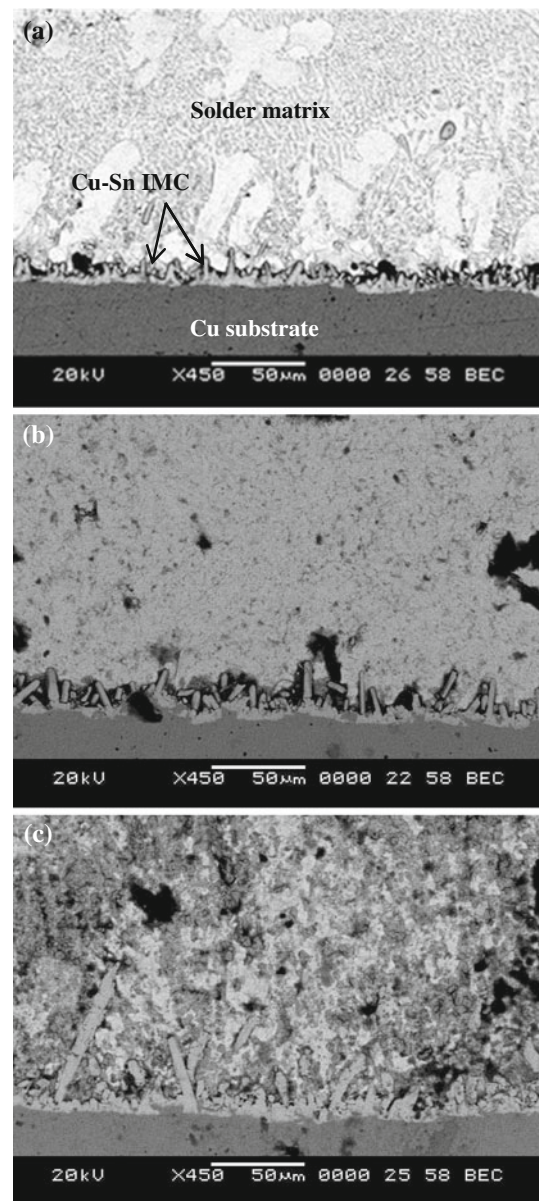


Fig. 5 SEM micrographs of solder solidified on rough Cu surface at **a** 240 °C, **b** 260 °C and **c** 280 °C reflow temperatures

Table 2 Effect of reflow temperature and substrate surface rough on IMCs formed between solder and Cu substrate

Nature of substrate surface	Temperature (°C)	Mean length (μm)	Mean thickness (μm)
Smooth	240	28	5
	260	32	5
	280	38	5
Rough	240	14	3
	260	16	5
	280	23	7

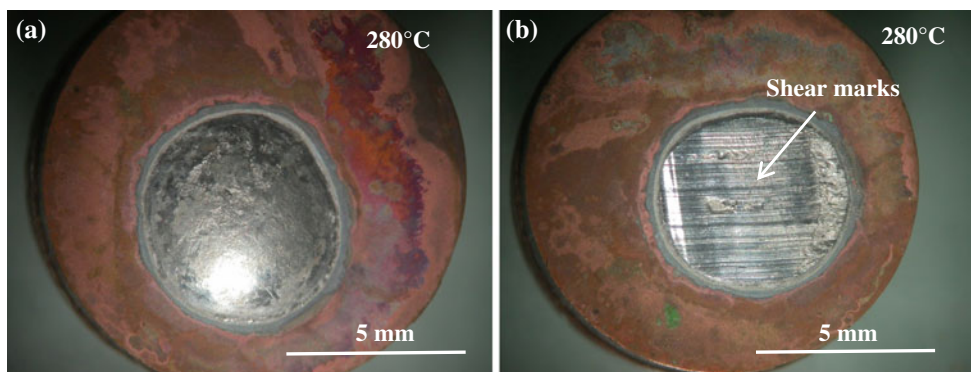


Fig. 6 **a** Macroscopic image (*top view*) of stabilized solder on smooth Cu surface, **b** Macroscopic image (*top view*) of sheared solder on smooth Cu surface

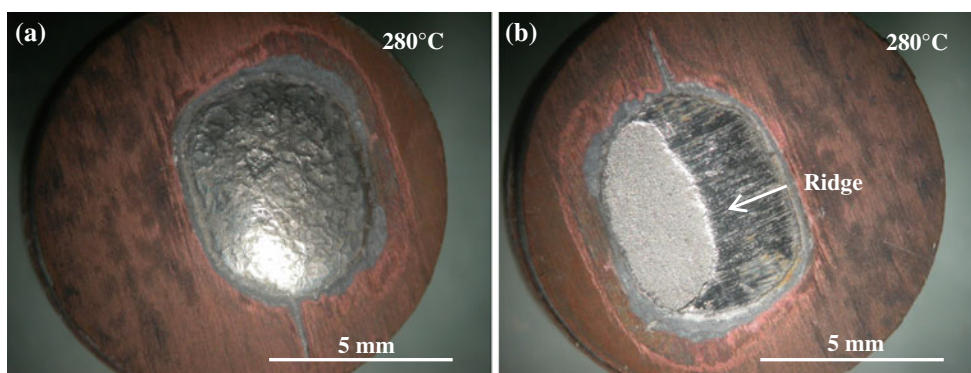


Fig. 7 **a** Macroscopic image (*top view*) of stabilized solder on rough Cu surface, **b** Macroscopic image (*top view*) of sheared solder on rough Cu surface

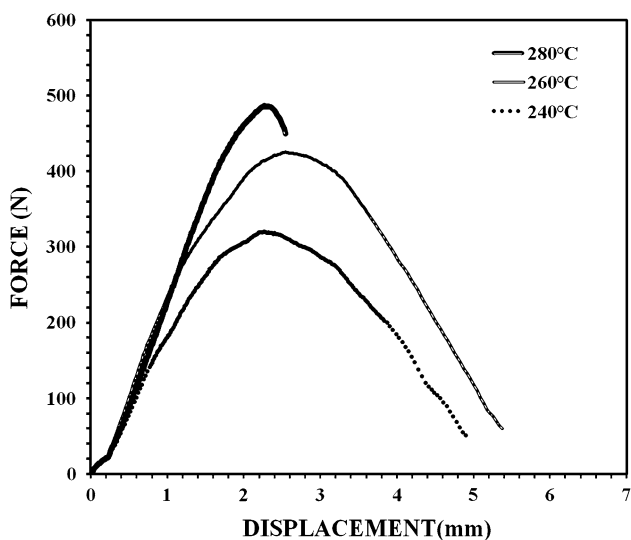


Fig. 8 Force versus displacement curves for solder bond on smooth Cu substrates reflowed at different temperatures

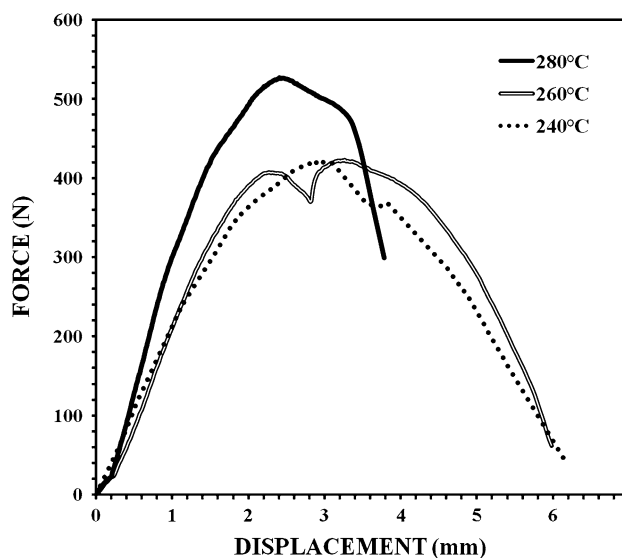


Fig. 9 Force versus displacement curves for solder bond on rough Cu substrate reflowed at different temperatures

β -Sn matrix. Ag_3Sn is likely to be formed even in the presence of 0.1 % Ag [24]. Fine dispersion of strips, rods or hollow tubes of Cu_6Sn_5 and Ag_3Sn IMC particles in the eutectic phase increases the shear strength of the alloy.

The variation in the shear force and shear energy for the solder bond on smooth and rough Cu could be explained in terms of the morphology and growth of intermetallic layer

Fig. 10 SEM micrographs of fractured surfaces of solder **a** smooth Cu substrate **b** rough Cu substrate

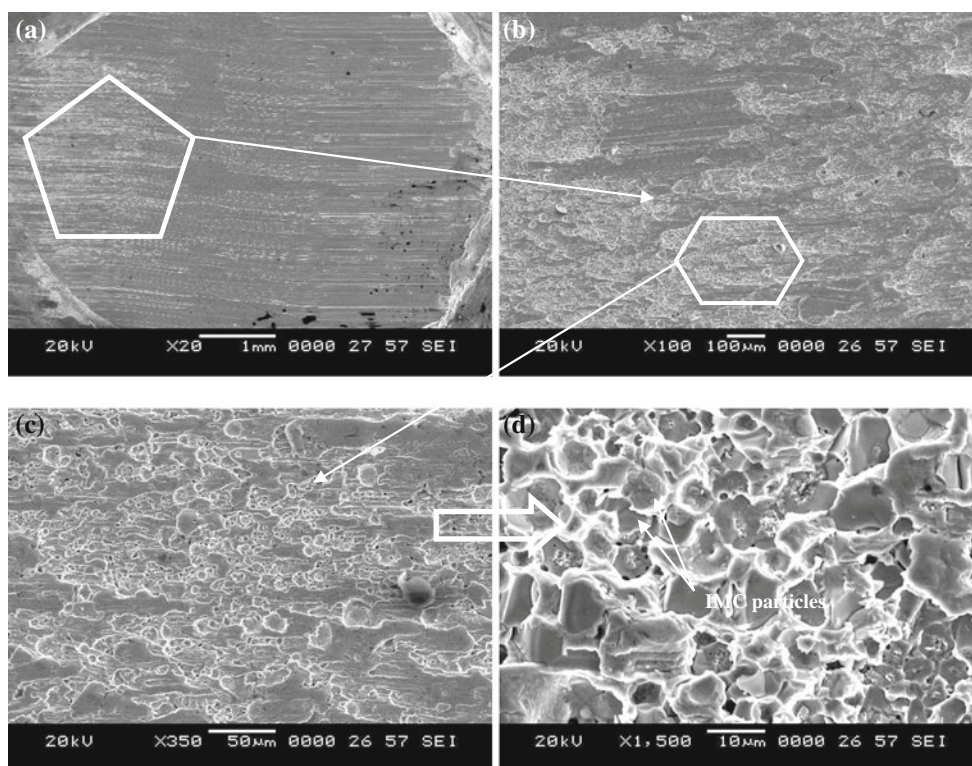
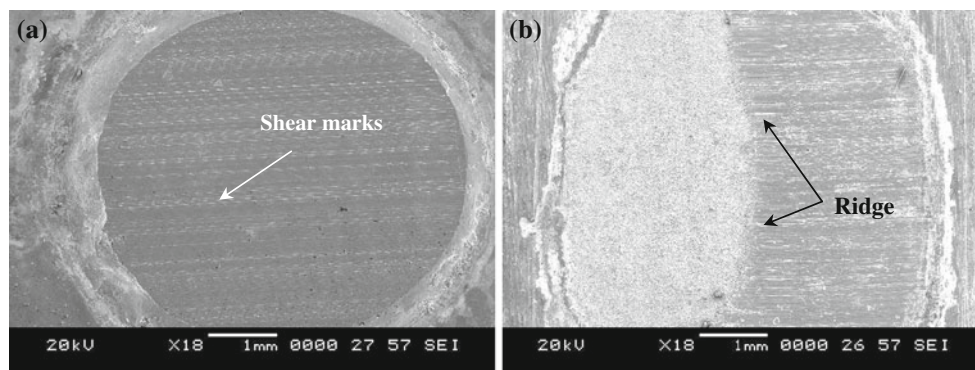


Fig. 11 SEM micrographs of fractured surfaces of solder on smooth Cu substrates

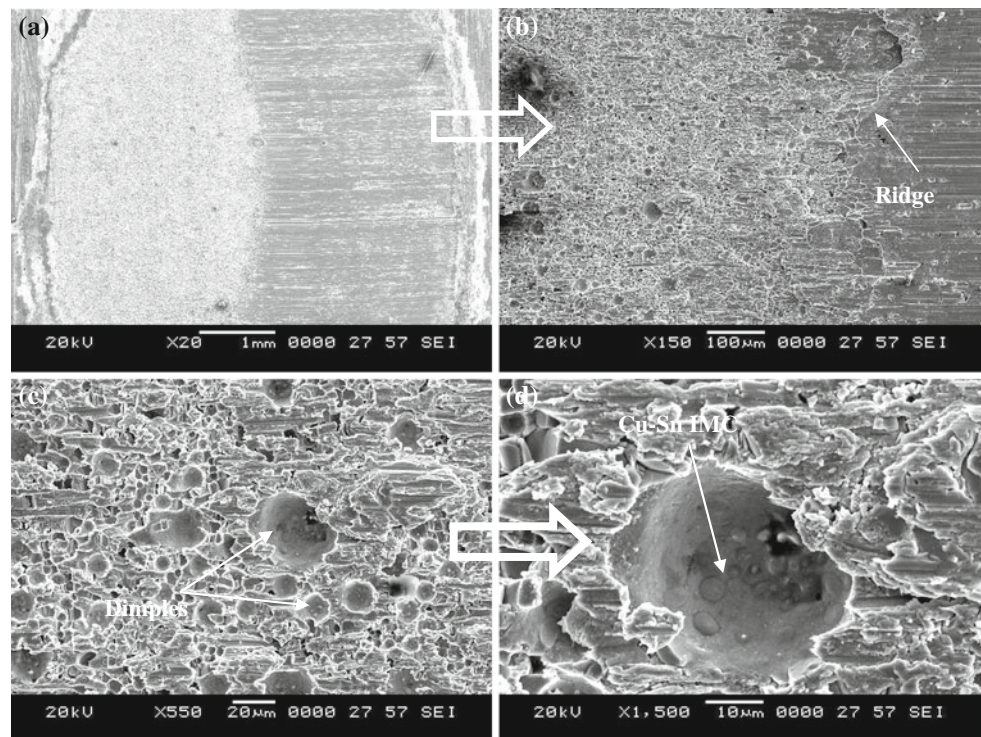
formed at the interface. At lower reflow temperatures, IMCs have not grown sufficiently to withstand the shear load. Hence, solder bond exhibited lower shear force at lower reflow temperatures. However, at higher reflow temperatures these sufficiently grown IMCs resist shear load leading to higher shear strength of the solder bond. Hence, at higher reflow temperatures, solder alloy exhibited higher shear force and shear energy.

Wettability of the solder alloy on rough Cu surfaces was found to be better than that on smooth Cu surfaces. Improved wettability of solder alloy implies increased reactivity of Cu atoms with liquid solder leading to ripening of the Cu_6Sn_5 IMC phases at the solder/rough-Cu interface. Generally during a shear test, when the shear tool

is in contact with the ripened and smooth Cu_6Sn_5 IMC layer, a higher shear force results. However, in the present study, a smooth IMC layer with short needles, were found at the interface of solder/Cu rough surface. The smooth surface resulted in a coarse IMC layer with long needles. Therefore, the solder alloy solidified on the rough surface yielded higher shear strength compared to smooth Cu surface.

Figure 11 shows the magnified view of SEM image of fractured surface of solder bond on smooth Cu surface. Fractured surfaces exhibited dimples as shown in Fig. 11c. The Cu_6Sn_5 needle shaped IMCs that are intact to the shear tool were observed inside the dimples of the fractured surfaces (Fig. 11d). Hence, on smooth substrates solder

Fig. 12 SEM micrographs of fractured surfaces of solder on rough Cu substrates



bond fractured predominantly in the solder matrix at different reflow temperatures. EDS analysis indicated that, the precipitates found inside the dimples were of Cu_6Sn_5 . The needle and plate like Ag_3Sn IMCs observed in the solder matrix and at the interface were completely sheared off.

Figure 12 shows the SEM micrographs of fractured solder bond on rough Cu surface. Figure 12b shows a magnified view of a transition ridge at which the fracture mode shifts from the solder to the interface region. Surprisingly, dimples were also found in the fractured surface. Dimples were more dominant at the fractured surface on rough surface as compared to that on smoother surface. This is due to the fracture of coarsened Cu-Sn IMC particles at the interface. Hexagonal Cu_6Sn_5 IMCs can be seen clearly at the center of each dimple (Fig. 12d).

During the shear test for the solder bond on rough substrate, the stress induced will be higher than smooth substrate. These higher concentrated stresses accumulated at the ridge. Once the load taken by the shear tool exceeds the higher concentrated stresses accumulated at the ridge, than the ductile failure mode changes to interfacial failure mode. Most of the needle shaped Cu_6Sn_5 IMCs fractured inside the dimples on fractured surface of solder bond on rough Cu substrate. Figure 12d confirms that the failure occurred at the interface.

According to Kim et al. [3], the presence of large Ag_3Sn platelets does not degrade strength directly, but affects the fracture mode. Large Ag_3Sn platelets induce brittle fracture

at the interface and provide crack initiation sites. Thus, large plate like Ag_3Sn IMCs precipitated at the interface could be the other reason for the interfacial failure.

Although shear force and shear energy values were found to be higher for the solder bond on rough surface, it is preferable to use smoother surface due to its predominant joint failure in the solder matrix.

4 Conclusion

Effect of reflow temperatures and substrate surface roughness on wettability, interfacial reactions and shear strength of SAC 387 solder alloy solidified on Cu substrates was assessed. Increase in reflow temperature and substrate surface roughness enhanced the wettability of the solder alloy. The size of needle shaped Cu_6Sn_5 IMCs increased with increase in temperature. The morphology of IMCs transformed from long to short needles with increase in substrate roughness. Shear strength and shear energy of the solder alloy were found to be higher on rough Cu surfaces than that on smooth Cu surfaces. However, the solder bond on rough Cu surface exhibited a transition ridge characterised by sheared IMCs whereas solder bond on smooth substrate surfaces exhibited completely ductile failure. Although, rough surface exhibited higher shear strength and shear energy, smoother surface is preferred due to its predominant joint failure occurring in the solder matrix.

Acknowledgments One of the authors (KNP) thanks the Defence Research Development Organisation, Government of India, New Delhi, for funding this research work under an R & D project (No. ERIP/ER/1006009M/01/1356).

References

1. A. Kroupa, D. Andersson, N. Hoo, J. Pearce, A. Watson, A. Dinsdale, S. Mucklejohn, *JMEPEG* **21**, 629 (2012)
2. J.S. Hwang, *Implementing Lead-Free Electronics* (McGraw-Hill, New York, 2005), pp. 1–40
3. K.S. Kim, S.H. Huh, K. Suganuma, *J. Alloys Compd.* **352**, 226 (2003)
4. J. Liang, S. Downes, N. Daravach, D. Shanggaun, S.M. Heinrich, *J. Electron. Mater.* **33**(12), 1507 (2004)
5. J.W. Yoon, S.W. Kim, S.B. Jung, *J. Alloys Compd.* **392**, 247 (2005)
6. H.H. Jiun, E.P. Leng, M. Ding, I. Ahmad, *Proceedings of 31st International Conference on Electronics Manufacturing and Technology*, (Petaling Jaya, 2007), p. 450
7. I. Ahmad, A. Jalar, B.Y. Majlis, R. Wagiran, *Int. J. Eng. Technol.* **4**(1), 123 (2007)
8. F. Song, S.W.R. Lee, K. Newman, S. Clark, B. Sykes, 9th Electronics Packaging Technology Conference, 450 (2007)
9. J.H.L. Pang, B.S. Xiong, *IEEE Trans. Compon. Packag. Technol.* **28**(4), 830 (2005)
10. F.X. Che, J.H.L. Pang, *J. Alloys Compd.* **541**, 6 (2012)
11. S.J. Hitchcock, N.T. Carroll, M.G. Nicholas, *J. Mater. Sci.* **16**, 714 (1981)
12. M.J. Rizvi, Y.C. Chan, C. Bailey, H. Lu, M.N. Islam, B.Y. Wu, *J. Electron. Mater.* **34**(8), 1115 (2005)
13. M.J. Rizvi, C. Bailey, Y.C. Chan, H. Lu, *J. Alloys Compd.* **438**, 116 (2007)
14. M.J. Rizvi, C. Bailey, Y.C. Chan, M.N. Islam, H. Lu, *J. Alloys Compd.* **438**, 122 (2007)
15. J.W. Yoon, B.I. Noh, B.K. Kim, C.C. Shur, S.B. Jung, *J. Alloys Compd.* **486**, 142 (2009)
16. M.J. Bozack, J.C. Suhling, Y. Zhang, Z. Cai, P. Lall, *J. Electron. Mater.* **40**(10), 2093 (2011)
17. H. Zhao, D.R. Nalagatla, D.P. Sekulic, *J. Electron. Mater.* **38**(2), 284 (2009)
18. T. Novak, F. Steiner, *Electronic Technology, ISSE 2009*, 32nd International Spring Seminar (13–17 May 2009)
19. W.K. Hsiao, *Effects of Surface Properties on Solder Bump Formation by Direct Droplet Deposition*, Ph. D Thesis 2004, Massachusetts Institute of Technology
20. Y.Y. Chen, J.G. Duh, *J. Mater. Sci.: Mater. Electron.* **11**, 279 (2000)
21. S.J. Hitchcock, N.T. Carroll, M.G. Nicholas, *J. Mater. Sci.* **16**, 714 (1981)
22. Satyanarayan, K.N. Prabhu, *J. ASTM Int* **7**(9), (2010) Paper ID JAI103052, 1
23. G. Kumar, K.N. Prabhu, *Adv. Colloid Interface Sci.* **133**, 61 (2007)
24. S.-H. Huh, K.-S. Kim, K. Suganuma, *Mater. Trans.* **42**(5), 739 (2001)